Development of a Variable Test Section Low Speed Wind Tunnel

A.K. Muchiri[1], B.Oindi[1], C. Soi[1]

Abstract—This paper will describe the process of developing a open-circuit low speed wind tunnel with a variable test section. The tunnel has a test chamber measuring 0.44m by 0.44m, with a varying length of between 0.5m and 0.9m. The maximum wind velocity attainable is to be 50m/s. The pressure drop inside the test section has been selected in order to suit the performance of an axial fan that is available at the institution. After fabrication, tests were run and the maximum velocity attained at the exit of the test section was 39.5m/s. Higher velocities can be attained if leakages within the test section and the diffuser are addressed. The tunnel is still under development, and the next phase is to install a Laser Doppler Velocimeter, profile the wall boundary layer profiles and a force balance to conduct experiments.

Keywords—Low speed wind tunnel, open-cicuit wind tunnel, wind tunnel test section

I. INTRODUCTION

WIND tunnels have been used in the field of aerodynamics for many decades now. They offer a good alternative to the actual testing of flow designs. Scale models of actual profiles to be tested are mounted inside a test section. Some of the parameters sought after include the drug coefficient, lift, moments and flow distribution.

Tunnels are normally classified according to the operation speeds, configuration and operating temperatures. Using the Mach number, Low-Speed flights and tunnels operate under Mach 0.33. Dimensionless numbers are used to match testing conditions.

Figure 1 illustrates the part of an open circuit wind tunnel.

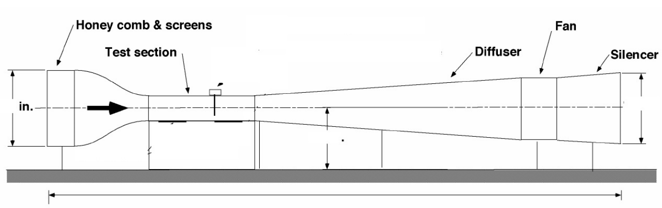

Fig. 1. Parts of an open-circuit low speed wind tunnel

II. THE TEST SECTION

The process of designing a wind tunnel starts at the test section. All other parts are then designed to conform to the requirements set for the test section.

A desired cross-section (α_T) and velocity (V_T) are selected. The selection is normally based on a multitude of factors, amongst which the size of models to be tested, and the environment in which the tunnel will be working. A hydraulic diameter is then determined.

$$D_T = 2\sqrt{\frac{A}{\pi}} \tag{1}$$

For a squared cross-section with each side measuring $0.44m$, the hydraulic diameter will be $0.4965m$.

The length of the test section should lie between 0.5 to 3 times the hydraulic diameter. A longer length would result is a large boundary layer formation that would eventually detach from the walls. Figure 2 shows the test section design

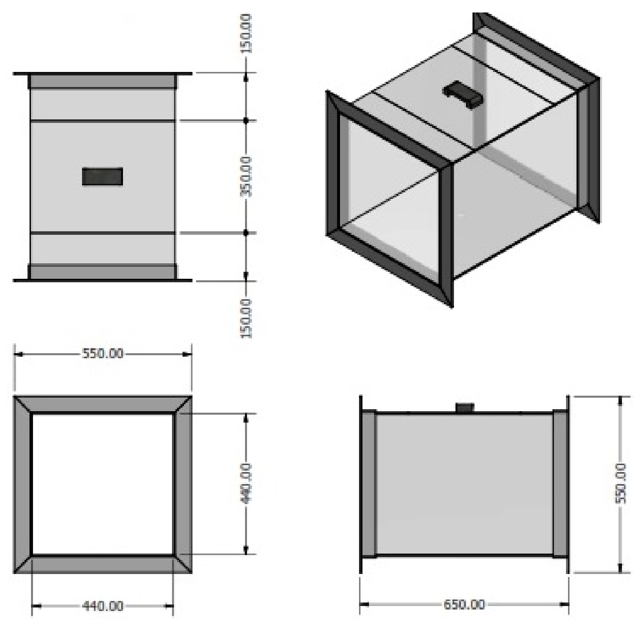

Fig. 2. Wind tunnel test section

III. THE INLET, SETTLING CHAMBER AND HONEYCOMB

The general arrangement of the settling chamber consists of a honeycomb, followed by screens. However, an initial mesh with wide spacing is normally placed at the entrance in order to block of items that may be sucked in by the inflow into the tunnel. This mesh has a very small impact on the reduction of swirls in the flow

A. Honeycombs and mesh

The two most effective turbulence manipulators are honeycomb and mesh screens, each of which serves a specific

[1]A.K. Muchiri, Department of Mechatronic Engineering, JKUAT (phone: +254722217209; fax: +2546752711; e-mail: muchiri@eng. jkuat.ac.ke).
B.O. Namasege, Department of Mechatronic Engineering, JKUAT
Caleb Soi, Department of Mechatronic Engineering, JKUAT

purpose. Honeycombs are located in the settling chamber, and are used to reduce non-uniformities in the flow. They should be 6-8 cell diameters thick, and cell size should be on the order of about 150 cells per settling chamber diameter.

1) Spacing of screens: The spacing of screens is based on two important properties:

1) Recovery of static pressure:
   For an independent pressure drop through the screens, spacing should be such that the static pressure has fully recovered from perturbation before reaching the next screen.
   $$\frac{dp}{dy} = 0 \tag{2}$$
2) Energy and eddies:
   In order to benefit fully from turbulence reduction, the minimum spacing should be of the order of the large energy containing eddies.

B. Design

Based on the size of the entrance of the contraction section, which is a square shape measuring $1210mm \times 1210mm$, the hydraulic diameter can be calculated to be:

$$D_H = 2\sqrt{\frac{A}{\pi}} = 2 \times \sqrt{\frac{14464100}{\pi}} = 1,366.217mm$$

Hence

$$0.2 \times 1366.217mm = 273.2444mm \approx 275mm$$

The mesh before the start of the contraction chamber will be at a distance of 275mm. This mesh should have a spacing of between 0.5mm-2.0mm The next mesh will be at 275mm upstream with spaces of 2mm-5mm. The Honeycomb will be 275mm further upstream. The thickness of the honeycomb will be 100mm. Finally, a mesh with spaces of 5mm- 10mm will be placed just before the honeycomb.
Effectively, the total length of the settling chamber will therefore be 1025mm. This includes an allowance of 100mm for the rounding of the inlet
The honeycomb will be 6-8 cell diameters thick, and the cell size in the order of 150 cells per settling chamber diameter. A thickness of 100mm is chosen for a cell diameter of 15mm.

C. The contraction

This section comes after the settling chamber and connects to the test section. Its main purpose is to increase the mean velocity of the flow at the entrance of the test section. It also helps to moderate any inconsistencies that may affect the uniform flow. A large area ratio of the entrance and exit of the contraction section is preferable, since it reduces the power loss across the screens, and the thickness of the boundary layer. However, for small tunnels, a ratio of between 6 - 9 is used [?], [?].

1) Designing the contraction section: The contraction wall shape profile consists of two elliptical arcs, matching at a point, which is the maximum slope. The profile is not a regular shape, and hence it requires to be estimated using a polynomial relationship. For wind tunnel contraction, the profile is determined using the Bell-Mehta's polynomial equation,

$$y = a\xi^5 + \xi^4 b + \xi^3 c + \xi^2 d + \xi e + f \tag{3}$$

where

$$\xi = \frac{x}{L} \tag{4}$$

L is the total axial nozzle length.
It has been established experimentally that the best ratio for $\frac{L}{2y_0}$ should be around the value 1. This is because,
- If $\frac{L}{2y_0} < 0.67$, the flow detaches from the wall
- If $\frac{L}{2y_0} > 1.79$, the boundary layer increases significantly.

Fixing one value such as y_0 will help determine the maximum value for L.
The inlet to outlet ratio is

$$\frac{1600^2}{440^2} = 7.5625 \tag{5}$$

Hence $y_0 = 605mm$. L will then take the value $2y_0$ which is 1210mm. Subsequently, the values for the contraction profile can be determined.

2) Contractor values used for fabrication: Fabrication facilities available do not allow for precise values to be achieved, as given on Table I. However, it is still possible to estimate the elliptical shape by working with values with a more reasonable resolution:

TABLE I
MODIFIED CONTRACTION VALUES

x	y
0	220
100	222
200	233
300	259
400	299
500	351
600	410
700	468
800	521
900	560
1000	590
1100	602
1200	605

IV. The Diffuser

The purpose if the diffuser is to reduce the power losses due to high flow velocity. The velocity of the flow must decrease with distance without any separation of boundary layers at walls. If separation occurs, vibrations would result. This would then interfere with the fan and measurements in the test section.
The divergence angle of the diffuser is determined using the relationship

$$\theta = \tan^{-1}\left(\frac{R_2 - R_1}{L}\right) = \tan^{-1}\left(\frac{1}{2}\frac{\sqrt{A_R} - 1}{L/D_1}\right) \quad (6)$$

Where $A_R = \frac{A_2}{A_1}$.
Equation 6 is also presented in graph form.
The contraction is made using galvanized steel plate. It has a circular cross-section and hence a transition is made from a square section to a circular section.
The diffuser has a constant divergence angle of 7.6^o between the upper and lower surface. Figure 3 shows the final 3D model of the tunnel developed.

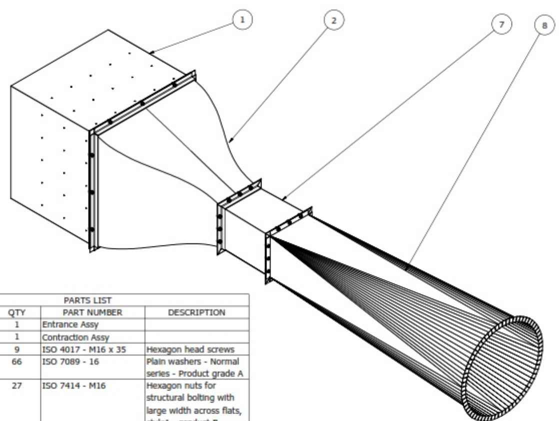

PARTS LIST			
ITEM	QTY	PART NUMBER	DESCRIPTION
1	1	Entrance Assy	
2	1	Contraction Assy	
3	9	ISO 4017 - M16 x 35	Hexagon head screws
4	66	ISO 7089 - 16	Plain washers - Normal series - Product grade A
5	27	ISO 7414 - M16	Hexagon nuts for structural bolting with large width across flats, style1 - product B - property class 10
6	6	ISO 4034 - M16	Hexagon nuts - Product grade C
7	1	test section ver2 assembli	
8	1	diffuser	

Fig. 3. Wind tunnel

V. Support structure

The support structure is meant to hold the entire tunnel together, and to raise it to a workable height. The height of the structure is determined by the ideal height of the test section. The base of of the test section is set at a height of 1500mm from the ground. Subsequently, the lowest point of the tunnel will be the inlet, with a clearance of 880mm, and a maximum height of 2,560mm.
The structure is made out of a 50mm x 50mm x 3mm L-beam. At the points of connection to the tunnel sections, rubber washers are used. These ensure that there is damping of vibration, so that the vibrations are not transferred to the environment.

VI. Drive section and Fan

This part refers to the air propulsion section. It consists of two parts, namely the motor, and the motor drive (Power supply and speed control).

A. The Motor

An axial fan driven by a 3-phase, 7.5hp, 1500rpm AC motor provides the power to the tunnel. The fan is mounted at the front of the tunnel, and drives air into the tunnel. The motor is mounted in the middle of the fan section, and connected to the fan via a coupling. A double rubber sealing is used to prevent vibrational motion during its operation.
The fan is made out of 12 vanes of 6mm thickness. No provision to change the blades is provided. Hence, a steel cage is built around it to prevent object ingestion that can damage the blades.
Mounting of the fan to the rest of the structure is very critical in that misalignment will lead to vibrations, that would interfere with the flow and measurements.

1) Power supply and motor speed control: In order to have a variable flow speed in the tunnel, power to the motor is provided via a frequency drive inverter, with settings from 0 - 50Hz. The motor rotates at 1500 rpm when the frequency is at 50Hz.

VII. Results and discussion

The wind tunnel was fabricated and preliminary tests were conducted to determine the maximum velocities achievable. Figure X shows the fabricated low-speed tunnel. Table II

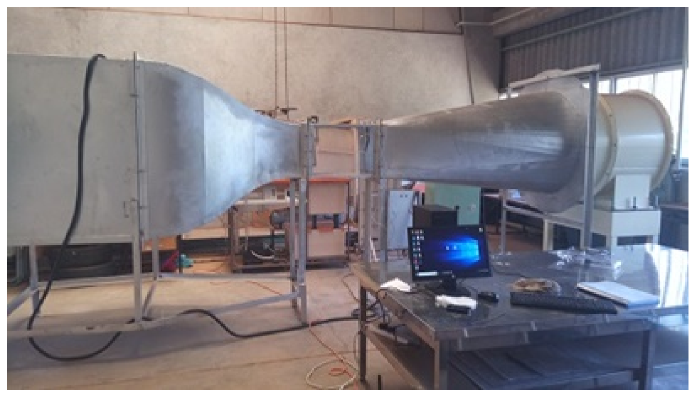

Fig. 4. Fabricated wind tunnel

shows how the measurements varied as the inverter frequency was varied from 15 Hz to 50Hz. These results are also

TABLE II
Temperature and velocity measurements in test section at varying inverter frequencies

Frequency (Hz)	Pitot-Tube Voltage	Pressure Difference	Velocity (m/s)	Thermistor Voltage	Temperature (^oC)
15	4.340088	0.8437835	27.38699	4.4062585	23.6917
20	5.2085925	1.033177	31.81089	4.4257315	24.6081
25	4.82032	1.040833	32.28604	4.434391	24.8819
30	4.503571	1.037866	33.5887	4.435769	24.5576
35	4.6466185	1.0944265	34.9965	4.479379	23.2329
40	4.631292	1.125051	36.23238	4.444965	25.7356
45	4.626183	1.158228	37.34062	4.4915855	24.4899
50	4.6517275	1.216926	39.21336	4.4309005	21.9713

illustrated on figure 5 It can be seen that the maximum velocity obtained was 39.21m/s. The minimum velocity achieved was a bit high. The measurements were confirmed using an anemometer.
It was not possible to characterize the flow throughout the tunnel due to the limitation of using a static pitot tube. It was also observed that there were pressure leakages around the test section, and that the end-part of the diffuser.

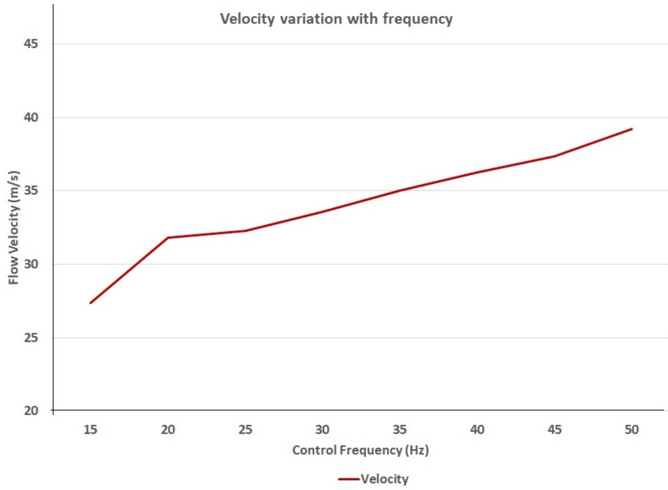

Fig. 5. Velocity against frequency setting

VIII. Conclusion and way forward

The developed wind tunnel allows for variation of the test section, hence giving a researcher the option to vary the size of the test model. Further development of the tunnel is ongoing to reduce the leakages experienced, and aim at increasing the flow velocity to a maximum of 70m/s. Characterization of the flow inside the entire test section is necessary to establish the boundary layer behaviour, and points at which turbulence may occur.

Acknowledgment

The authors would like to thank Africa-ai-Japan Project (Phase 1 & Phase 2) for their continued support towards the realization of this project